Excitation of Multiple Dipole Surface Plasmon Resonances in Spherical Silver Nanoparticles Embedded in a Highly Dispersive Medium

Bjoern Niesen,[*,†,‡] Barry P. Rand,[†] Pol Van Dorpe,[†,‡] Honghui Shen,[¶] Bjorn Maes,[¶] Jan Genoe,[†] and Paul Heremans[†,‡]

imec, Kapeldreef 75, B-3001 Leuven, Belgium, Department of Electrical Engineering (ESAT), Katholieke Universiteit Leuven, Kasteelpark Arenberg 10, B-3001 Leuven, Belgium, and Department of Information Technology (INTEC), Photonics Research Group, Ghent University-imec, St-Pietersnieuwstraat 41, 9000 Ghent, Belgium

E-mail: Bjoern.Niesen@imec.be

KEYWORDS: Metal nanoparticle, surface plasmon, dipole resonance, organic semiconductor, permittivity, absorption enhancement

Abstract

We observe the appearance of multiple dipole surface plasmon resonances in spherical Ag nanoparticles when embedded in an organic semiconductor that exhibits a highly dispersive permittivity. Comparing the absorption spectra of thin-films with and without Ag nanoparticles reveals the presence of two plasmon peaks. Numerical simulations and calculations based

[*]To whom correspondence should be addressed
[†]imec, Kapeldreef 75, B-3001 Leuven, Belgium
[‡]Department of Electrical Engineering (ESAT), Katholieke Universiteit Leuven, Kasteelpark Arenberg 10, B-3001 Leuven, Belgium
[¶]Department of Information Technology (INTEC), Photonics Research Group, Ghent University-imec, St-Pietersnieuwstraat 41, 9000 Ghent, Belgium

on an electrostatic model allow to attribute both peaks to dipole resonances, and show that the strong dispersion of the organic permittivity is responsible for this behavior. The presence of these two plasmon resonances was found to enhance the absorption of the organic semiconductor over a broad wavelength range, and in particular in the red absorption tail.

Metal nanoparticles (NPs) possess unique optical properties that arise from the collective oscillations of their free electrons when they are excited by an electromagnetic wave. The strength and frequency of this so-called localized surface plasmon resonance (LSPR) does not only depend on the metal NP size and shape, but is also highly sensitive to changes in the dielectric environment.[1–5] These properties give metal NPs potential applications in sensors,[6–8] photovoltaic cells,[9–13] light emitting devices,[14,15] and surface-enhanced Raman scattering spectroscopy.[16,17]

When a spherical metal NP is irradiated with light of a wavelength much larger than the particle radius R, it can be assumed that the NP is exposed to a spatially constant electromagnetic field and therefore only dipole LSPRs are excited.[18,19] According to this quasi-static approximation, the NP can be described as an ideal dipole with polarizability $\alpha(\omega)$ given by

$$\alpha(\omega) = 4\pi\varepsilon_0 R^3 \frac{\varepsilon_{\mathrm{NP}}(\omega) - \varepsilon_{\mathrm{m}}(\omega)}{\varepsilon_{\mathrm{NP}}(\omega) + 2\varepsilon_{\mathrm{m}}(\omega)} , \tag{1}$$

where ε_0 is the vacuum permittivity and ω the frequency of the incident electromagnetic wave, and $\varepsilon_{\mathrm{NP}}(\omega)$ and $\varepsilon_{\mathrm{m}}(\omega)$ denote the relative permittivity of the metal NP and the embedding medium, respectively. In general, both relative permittivities are complex numbers with $\varepsilon(\omega) = \varepsilon_1(\omega) + i\varepsilon_2(\omega)$. From Eq. 1, it follows that resonances can be excited, given that at the resonance frequencies the embedding medium absorbs weakly (i.e. $\varepsilon_{2,\mathrm{m}}(\omega) << 1$), and $\varepsilon_{2,\mathrm{NP}}(\omega)$ or $\partial\varepsilon_{2,\mathrm{NP}}(\omega)/\partial\omega$ are small. These resonances can then occur if

$$\varepsilon_{1,\mathrm{NP}}(\omega) = -2\varepsilon_{1,\mathrm{m}}(\omega) . \tag{2}$$

For a spherical metal NP in most embedding media, this dipole resonance condition is typically fulfilled once, either in the ultraviolet, visible or near-infrared wavelength range.

Here, however, we show that for spherical metal NPs in highly dispersive media, multiple dipole LSPRs can occur. As highly dispersive medium we chose chloro[subphthalocyaninato]boron(III) (SubPc), an organic semiconducting molecule with very strong absorption in limited absorption bands and applications in organic solar cells.[20,21] We compare the light absorption of thin-films consisting of Ag NPs embedded in SubPc with that of pure SubPc thin-films, indeed revealing not one, but two additional absorption bands due to the Ag NPs. By considering the relative permittivities of Ag and SubPc as well as numerical simulations that show excellent agreement with our experimental results, we are able to attribute the absorption in the Ag NPs at both bands to dipole LSPRs. The possibility of obtaining multiple dipole LSPR absorption bands from spherical metal NPs has to our knowledge not been considered before. We propose its application for enhancing the absorption in organic photovoltaic cells and photodetectors.

Thin-films were deposited on glass (Corning Eagle XG) or Si/SiO_2 substrates by thermal evaporation at a chamber pressure below 2×10^{-6} Torr. A quartz-crystal oscillator was used to monitor the growth rate and the layer thickness. The substrates were rotated during deposition for better layer uniformity. Prior to deposition, the substrates were solvent cleaned followed by an ultraviolet/O_3 treatment for 15 min. Silver NPs were obtained by depositing Ag (99.99% purity, Kurt. J. Lesker Company) at 0.01 nm/s to a thickness of 1 nm, as determined by the quartz-crystal oscillator. SubPc (purchased from Sigma Aldrich) was purified twice by thermal gradient sublimation and deposited at 0.1 nm/s either directly on the substrate or on top of the Ag NP layer. The direct light transmission of thin-films on glass was measured using a Shimadzu UV-1601PC spectrophotometer, whereas the diffuse transmission and reflectance were measured using a Bentham PVE 300 photovoltaic device characterization system. As light scattering by the thin-films was found to be negligible (cf. Fig. S1 in Supporting Information), the light absorption was defined as absorption = 1 - direct transmission - reflectance. The absorption of the glass substrate was subtracted from all absorption spectra. Relative permittivities of SubPc and Ag were determined from thin-films on Si/SiO_2 substrates using a SOPRA GESP-5 spectroscopic ellipsometer. The morphology of Ag NPs was determined by scanning electron microscopy (Hitachi SU8000)

and atomic force microscopy in tapping mode (Veeco Dimension 3100 system with Nanoscope IV controller).

The deposition of 1 nm of Ag by thermal evaporation led to a dense layer of NPs as observed from the scanning electron micrograph in Fig. 1(a). From above, the NPs possess a circular shape, with an average particle diameter of 7 nm and an inter-particle spacing comparable to the particle size. From atomic force microscopy measurements [cf. Fig. 1(b)], an average NP height of 5 nm was determined. The absorption spectrum of the uncovered Ag NP layer is shown in Fig. 2(a) as a dashed curve and features a single band centered at a wavelength of $\lambda = 430$ nm. The small size of the Ag NPs compared to this wavelength allows to apply the quasi-static approximation to determine whether a dipole LSPR is expected at this spectral position. Indeed, from Eq. 2, a single resonance at $\lambda = 360$ nm is obtained for a spherical Ag NP in vacuum, using the relative permittivity of Ag shown in Fig. 3(a). The absorption band can therefore be attributed to a dipole LSPR, red-shifted from the calculated value due to the presence of the substrate, interactions between the NPs, and the deviation of the NP shape from a perfect sphere.[22,23] The absence of any further absorption bands is expected for Ag NPs of this size, and indicates that no higher order LSPR modes are excited.[24]

The absorption spectra of thin-films consisting of the Ag NP layer covered by 6 to 30 nm of SubPc are shown in Fig. 2(a) as solid curves, whereas the spectra of pure SubPc thin-films with the same thicknesses are shown in Fig. 2(b). In both cases, the strengths of the high energy Soret band ($\lambda = 320$ nm) and the low energy Q band (450 nm $< \lambda <$ 630 nm) increase with increasing SubPc layer thickness. In order to determine the impact of the presence of the Ag NPs to the absorption of these layers, each absorption spectrum of the pure SubPc layers was subtracted from that of the thin-film consisting of Ag NPs and SubPc with the same layer thickness. These absorption differences feature two bands centered at $\lambda = 445$ nm and $\lambda =$ 610-630 nm, as shown in Fig. 2(c). The intensity of both bands decreases with increasing SubPc thickness, with the largest spectral variations with thickness appearing at $\lambda > 500$ nm.

The analysis of this absorption difference is complicated by the fact that in addition to the

LSPRs in the Ag NPs, contributions from enhanced absorption in the SubPc layer via the increased electromagnetic field surrounding the NPs are expected.[25,26] Such a plasmonic absorption enhancement has already been reported for Ag NPs embedded in the organic semiconductor copper phthalocyanine.[11] The wavelengths at which the Ag NP LSPRs contribute to the absorption difference can be estimated by applying Eq. 2 for a spherical Ag NP embedded in SubPc. The relative permittivity of SubPc is shown in Fig. 3(b). It is highly dispersive, with its real ($\varepsilon_{1,\mathrm{SubPc}}$) and imaginary part ($\varepsilon_{2,\mathrm{SubPc}}$) featuring an intense peak at $\lambda = 603$ nm and $\lambda = 591$ nm, respectively, corresponding to the strong light absorption of SubPc at these wavelengths. Interestingly, as a result of this highly dispersive permittivity of SubPc, three wavelengths are obtained where Eq. 2 is satisfied, being at $\lambda = 430$, 592, and 624 nm [cf. Fig. 3(c)]. However, as $\varepsilon_{2,\mathrm{SubPc}}$ is large at $\lambda =$ 592 nm, the resonant behavior of $\alpha(\omega)$ is strongly damped at this wavelength (cf. Fig. S2 Supporting Information). Therefore, the two solutions of Eq. 2 at $\lambda = 430$ and 624 nm are expected to give rise to dipole LSPRs. This agrees well with the observed absorption differences, as shown in Fig. 3(c) for a SubPc thickness of 10 nm, and suggests that, indeed, dipole LSPRs contribute to both absorption bands.

In order to obtain further evidence for the nature of the absorption difference, numerical simulations were performed using COMSOL Multiphysics 3.5a. The geometry used for these three-dimensional simulations was motivated by our microscopy studies (cf. Fig. 1) and is shown as an inset in Fig. 4(b). A periodic two-dimensional array of truncated Ag spheroids with a height of 5 nm, a lateral dimension of 7 nm and a center-to-center spacing of 14 nm represent the Ag NPs. The SubPc layers coating these truncated Ag spheroids have a thickness of either 10, 14, 18, 22 or 30 nm and a flat horizontal surface. As a reference, pure SubPc layers with the same thicknesses were simulated. The light is incident through the semi-infinite glass substrate ($\varepsilon_1 = 2.25$, $\varepsilon_2 = 0$), with the propagation vector k parallel to the y-axis and the electric field E parallel to the x-axis. The light absorption in the Ag and in SubPc was monitored separately. For the pure SubPc layers the monitored area excluded the area corresponding to the truncated Ag spheroids, such that the same SubPc area was monitored for the layers with and without the Ag NPs.

The difference between the absorption in the SubPc covering the truncated Ag spheroids and the pure SubPc layer is plotted for each SubPc thickness in Fig. 4(a). These spectra show a broad band with two peaks at $\lambda = 452$ and 624 nm, and can be attributed to the plasmonic absorption enhancement in SubPc. The absorption in Ag is shown as solid curves in Fig. 4(b) for the truncated Ag spheroids covered by SubPc layers with different thicknesses. These spectra feature two distinct bands centered at $\lambda = 446$ and 632 nm. For the absorption in the Ag as well as for the absorption difference in SubPc, the intensity of all bands decreases with increasing SubPc layer thickness. In contrast to the experimentally observed absorption differences, the low energy band of the Ag absorption spectra obtained from these simulations is stronger than the high energy band. This could be due to damping of the low energy LSPR by the inhomogeneous size and shape distribution of the Ag NPs as well as by voids between the Ag NPs and the SubPc caused by shadowing during the SubPc deposition. Qualitatively, however, these results are well in agreement with the experimentally observed results and clearly confirm the presence of absorption enhancement in SubPc at wavelengths above the high energy LSPR as well as the presence of two plasmon resonances in the Ag NPs surrounded by SubPc. Furthermore, as observed experimentally, the low energy plasmon peak is not present in the case of the uncovered truncated Ag spheroid [cf. dashed curve in Fig. 4(b)]. Finally, the x and y component of the electric field surrounding the truncated Ag spheroid covered by 10 nm of SubPc shown in Fig. 4(c) confirm that both LSPRs are indeed dipolar in nature.

In summary, we observed two bands from the absorption difference between thin-films consisting of a Ag NP layer covered by SubPc and pure SubPc thin-films. By means of numerical simulations, plasmonic enhancement in the SubPc layer as well as absorption in the Ag NPs was found to contribute to both bands. By considering the simulated electric field surrounding the Ag NPs as well as calculations applying the quasi-static approximation, we were able to attribute the absorption in the Ag NPs at both absorption bands to dipole LSPRs. It should be further noted that the presence of multiple dipole resonances was not observed in the Ag NP layer without the SubPc medium surrounding it. Given this, we conclude that embedding spherical metal NPs in a highly

dispersive medium can give rise to multiple absorption bands originating from dipole resonances, which is otherwise only exhibited by non-spherical NPs,[27] and could be employed to broaden the spectral range of metal NP-based sensors. Furthermore, as the increase of absorption in SubPc benefits from the multiple LSPRs of the Ag NPs [cf. Fig. 4(a)], this feature is expected to find application in organic solar cells, where enhanced absorption in the red tail of the absorption spectra of the organic semiconductor should give rise to a corresponding increase in photocurrent.[28,29]

Acknowledgement

The authors gratefully acknowledge Josine Loo for obtaining scanning electron micrographs, Alain Moussa for obtaining atomic force micrographs, and David Cheyns for measuring optical constants. This work was supported by the European Community's Seventh Framework Programme under Grant No. FP7-ICT-2009-4-248154 ("PRIMA") and the Institute for the Promotion of Innovation by Science and Technology in Flanders (IWT) via the SBO-project No. 060843 ("PolySpec"). P.V.D. thanks the Fonds Wetenschappelijk Onderzoek Vlaanderen (FWO)-Flanders for financial support.

Supporting Information Available

Comparison between the direct and the diffuse light transmission for a thin-film consisting of Ag NPs and SubPc and for a pure SubPc thin-film, and the resonance behavior of the polarizability of a spherical Ag NP in SubPc. This material is available free of charge via the Internet at `http://pubs.acs.org/`.

References

(1) Noguez, C. *J. Phys. Chem. C* **2007**, *111*, 3806.

(2) Kelly, K. L.; Coronado, E.; Zhao, L. L.; Schatz, G. C. *J. Phys. Chem. B* **2003**, *107*, 668.

(3) Evanoff, D. D., Jr.; White, R. L.; Chumanov, G. *J. Phys. Chem. B* **2004**, *108*, 1522.

(4) Jain, P. K.; Lee, K. S.; El-Sayed, I. H.; El-Sayed, M. A. *J. Phys. Chem. B* **2006**, *110*, 7238.

(5) Mock, J. J.; Smith, D. R.; Schultz, S. *Nano Lett.* **2003**, *3*, 485.

(6) Anker, J. N.; Hall, W. P.; Lyandres, O.; Shah, N. C.; Zhao, J.; Van Duyne, R. P. *Nature Mater.* **2008**, *7*, 442.

(7) Daniel, M.-C.; Astruc, D. *Chem. Rev.* **2004**, *104*, 293.

(8) Haick, H. *J. Phys. D: Appl. Phys.* **2007**, *40*, 7173.

(9) Atwater, H. A.; Polman, A. *Nature Mater.* **2010**, *9*, 205.

(10) Hallermann, F.; Rockstuhl, C.; Fahr, S.; Seifert, G.; Wackerow, S.; Graener, H.; v. Plessen, G.; Lederer, F. *Phys. Status Solidi A* **2008**, *205*, 2844.

(11) Rand, B. P.; Peumans, P.; Forrest, S. R. *J. Appl. Phys.* **2004**, *96*, 7519.

(12) Morfa, A. J.; Rowlen, K. L.; Reilly III, T. H.; Romero, M. J.; van de Lagemaat, J. *Appl. Phys. Lett.* **2008**, *92*, 13504.

(13) Shen, H.; Bienstman, P.; Maes, B. *J. Appl. Phys.* **2009**, *106*, 073109.

(14) Choulis, S. A.; Mathai, M. K.; Choong, V.-E. *Appl. Phys. Lett.* **2006**, *88*, 213503.

(15) Kwon, M.-K.; Kim, J.-Y.; Kim, B.-H.; Park, I.-K.; Cho, C.-Y.; Byeon, C. C.; Park, S.-J. *Adv. Mater.* **2008**, *20*, 1253.

(16) Schlücker, S. *ChemPhysChem* **2009**, *10*, 1344.

(17) Han, X. X.; Zhao, B.; Ozaki, Y. *Anal. Bioanal. Chem.* **2009**, *394*, 1719.

(18) Kreibig, U.; Vollmer, M. *Optical Properties of Metal Clusters*; Springer: Berlin, 1995.

(19) Bohren, C. F.; Huffman, D. R. *Absorption and Scattering of Light by Small Particles*; Wiley Interscience: New York, 1983.

(20) Mutolo, K. L.; Mayo, E. I.; Rand, B. P.; Forrest, S. R.; Thompson, M. E. *J. Am. Chem. Soc.* **2006**, *128*, 8108.

(21) Gommans, H.; Cheyns, D.; Aernouts, T.; Girotto, C.; Poortmans, J.; Heremans, P. *Adv. Funct. Mater.* **2007**, *17*, 2653.

(22) Gupta, G.; Tanaka, D.; Ito, Y.; Shibata, D.; Shimojo, M.; Furuya, K.; Mitsui, K.; Kajikawa, K. *Nanotechnology* **2009**, *20*, 025703.

(23) Royer, P.; Bijeon, J. L.; Goudonnet, J. P.; Inagaki, T.; Arakawa, E. T. *Surf. Sci.* **1989**, *217*, 384.

(24) Kreibig, U.; Schmitz, B.; Breuer, H. D. *Phys. Rev. B* **1987**, *36*, 5027.

(25) Tanabe, K. *J. Phys. Chem. C* **2008**, *112*, 15721.

(26) Khurgin, J. B.; Sun, G. *J. Opt. Soc. Am. B* **2009**, *26*, B83.

(27) Sau, T. K.; Rogach, A. L.; Jäckel, F.; Klar, T. A.; Feldmann, J. *Adv. Mater.* DOI: 10.1002/adma.200902557.

(28) Rand, B. P.; Genoe, J.; Heremans, P.; Poortmans, J. *Prog. Photovolt: Res. Appl.* **2007**, *15*, 659.

(29) Thompson, B. C.; Fréchet, J. M. J. *Angew. Chem., Int. Ed.* **2008**, *47*, 58.

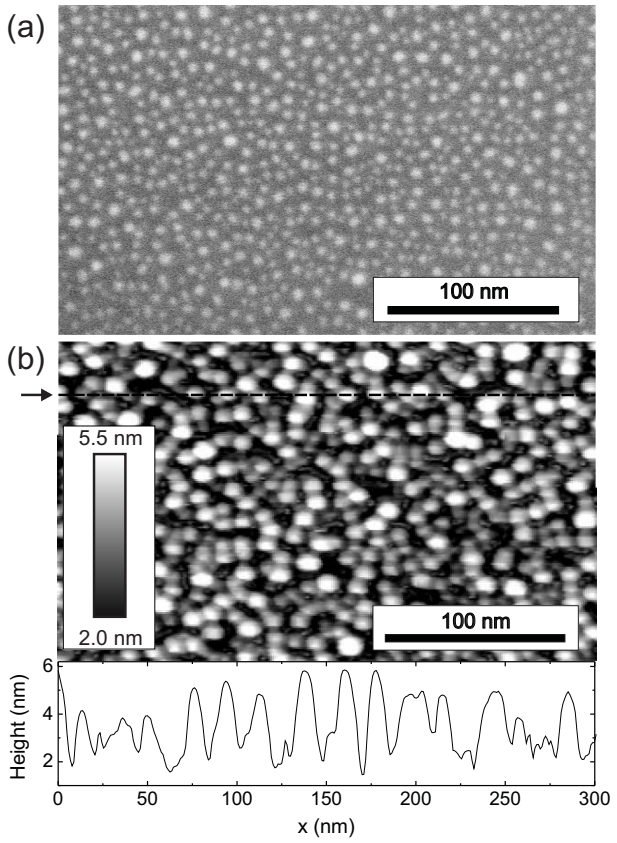

Figure 1: (a) Scanning electron micrograph of Ag NPs obtained by depositing 1 nm of Ag on a Si/SiO_2 substrate by thermal evaporation. From above, the particles have a circular shape with average diameter and inter-particle spacing of 7 nm. (b) Atomic force micrograph (top) of the Ag NPs on a glass substrate, with a height-profile (bottom) taken along the dashed line indicated by the arrow. An average NP height of 5 nm was determined from this micrograph. The lateral size of the NPs is overestimated due to convolution of the atomic force microscope tip and the sample features.

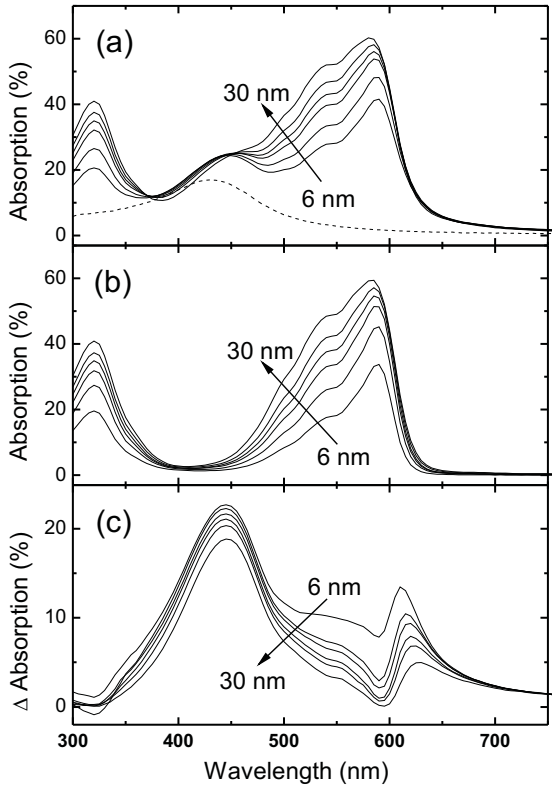

Figure 2: (a) Absorption spectra of uncoated Ag NPs on glass (dashed curve) and Ag NPs covered by SubPc with a layer thickness of 6, 10, 14, 18, 22, and 30 nm (solid curves). (b) Absorption spectra of SubPc layers on glass, with the same thicknesses as in (a). (c) Difference between the absorption spectra of thin-films containing SubPc and Ag NPs shown in (a) and those of pure SubPc layers shown in (b) for each SubPc layer thickness.

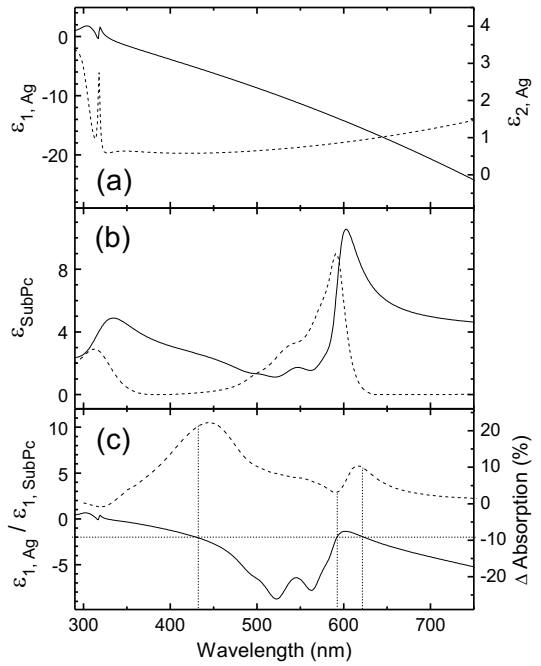

Figure 3: Real (ε_1, solid curve) and imaginary (ε_2, dashed curve) part of the relative permittivity of (a) Ag and (b) SubPc. The ratio $\varepsilon_{1,\mathrm{Ag}}/\varepsilon_{1,\mathrm{SubPc}}$ is plotted as solid curve in (c). For comparison, the dashed curve shows the absorption difference between a thin-film consisting of the Ag NP layer covered by 10 nm of SubPc and a pure SubPc layer with a thickness of 10 nm. The drop lines indicate the wavelengths where $\varepsilon_{1,\mathrm{Ag}}/\varepsilon_{1,\mathrm{SubPc}} = -2$.

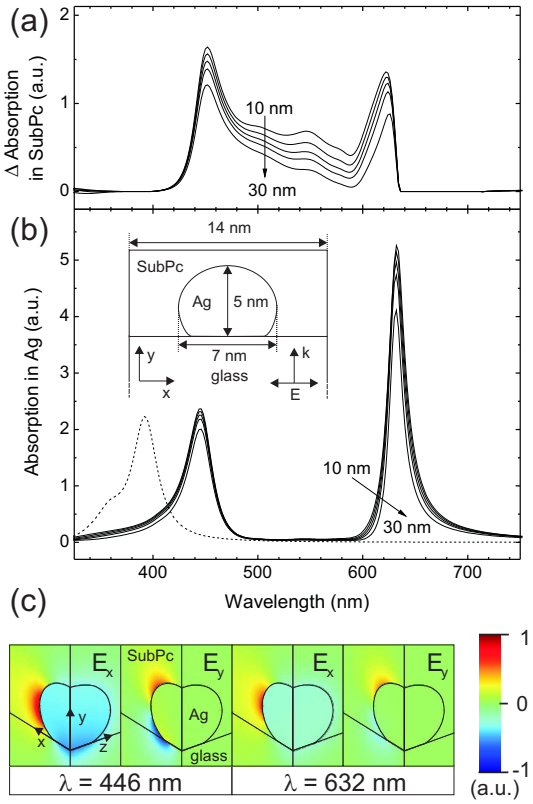

Figure 4: Results of three-dimensional numerical simulations performed using a geometry with a cross-section as shown in the inset in (b). Periodic boundaries in both lateral dimensions result in an infinite two-dimensional array of truncated Ag spheroids with center-to-center spacing of 14 nm. The light wave is incident through the glass substrate with the propagation vector k and electric field vector E as indicated by arrows. (a) Difference between the absorption in the SubPc layers with thicknesses of 10, 14, 18, 22, and 30 nm covering the truncated Ag spheroid and the absorption in pure SubPc layers (excluding the area corresponding to the truncated Ag spheroid) with the same thicknesses. (b) Absorption in the uncovered truncated Ag spheroid (dashed curve) and in the truncated Ag spheroid covered by SubPc layers with the same thicknesses as in (a) (solid curves). (c) Surface plots of the x and y component of the electric field at $\lambda = 446$ and 632 nm for a SubPc thickness of 10 nm.

Graphical TOC Entry